# A Collaborative Deployment Method of UAV Hangar Siting for Forest Inspection

*QIAN Long*[1], *LIU Jixin*[1,2*], *JIANG Hao*[1*], *ZENG Weili*[1,2], *YANG Zhao*[1,2]

1. College of Civil Aviation, Nanjing University of Aeronautics and Astronautics, Nanjing 211106, P. R. China;
2. State Key Laboratory of Air Traffic Management System, Nanjing 211106, P. R. China

(Received 23 October 2025; revised 23 April 2026; accepted 7 May 2026)

**Abstract:** The deployment of unmanned aerial vehicle (UAV) hangars is critical to the efficiency of forest inspections, significantly influencing both infrastructure construction costs and operational expenses. Existing research on hangar selection often overlooks the complex constraints posed by forest environments, such as topographical variability, power limitations, and coverage demands. To tackle these challenges, this paper presents a multi-objective optimization approach for UAV hangar selection in forest environments, aiming to reduce construction costs while maximizing coverage under complex topographical constraints. The process begins with the preliminary selection of candidate hangars, utilizing geographic data such as the digital elevation model (DEM), meteorological data, and power/signal coverage. A multi-criteria decision analysis (MCDA) method evaluates and scores candidates based on rigid and flexible criteria, including topographical suitability, wind speed, and power supply availability. A multi-objective optimization model is then developed to optimize the layout of hangars, incorporating critical constraints such as topographical characteristics, UAV power limits, and coverage redundancy. To solve this optimization problem, the non-dominated sorting genetic algorithm Ⅱ (NSGA-Ⅱ) is applied. Experimental results demonstrate that the proposed method outperforms traditional approaches, such as the greedy algorithm and the single-objective genetic algorithm. Specifically, the NSGA-Ⅱ method reduces the number of hangars by 8.3%, and increases the coverage by 1.6%. It also significantly accelerates the convergence, demonstrating superior performance and efficiency. This methodology provides a comprehensive solution for UAV deployment in forest inspections and can be adapted to other complex topography.

**Key words:** forest inspection; unmanned aerial vehicle (UAV) hangar deployment; multi-criteria decision analysis (MCDA); topographical constraints; multi-objective optimization

**CLC number:** V355 **Document code:** A **Article ID:** 1005-1120(2026)03-0371-15

## 0 Introduction

In recent years, unmanned aerial vehicle (UAV) technology has experienced remarkable advancements in flight control, navigation technologies, and operational endurance[1-3]. Consequently, application scenarios have expanded significantly, particularly in electric vertical take-off and landing (eVTOL) vehicles, logistics, and dedicated infrastructure development. This paper focuses on the collaborative optimization of hangars for multi-UAV deployment in forest inspection. Traditional forest monitoring, relying on ground rangers[4], satellite remote sensing[5], and fixed-wing aircraft, exhibits substantial limitations, such as restricted coverage and vulnerability to topographical constraints[6]. Conversely, UAVs offer rapid deployment and exceptional mobility, rendering them ideal for complex mountainous regions.

As UAV technologies progress, hangar selection has emerged as a pivotal research area. These points serve as critical nodes for charging, mission reconfiguration, and coordination. Existing research on UAV hangar deployment has predominantly

*Corresponding authors, E-mail addresses: larryljx66@nuaa.edu.cn; jianghao_cca@nuaa.edu.cn.

**How to cite this article**: QIAN Long, LIU Jixin, JIANG Hao, et al. A collaborative deployment method of UAV hangar siting for forest inspection[J]. Transactions of Nanjing University of Aeronautics and Astronautics, 2026, 43(3): 371-385.

http://dx.doi.org/10.16356/j.1005-1120.2026.03.004

evolved across three structured domains, material transportation[7-9], electric power inspection[10-13], and road inspection[14-17].

In the domain of material transportation, Wang et al.[7] and Murray et al.[8] developed logistics distribution models centered on range constraints and vehicle-UAV collaboration. However, these methodologies predominantly prioritize economic costs through single-objective models, which inherently neglect the synergistic effects and coverage redundancy between multiple hangars. Cheng et al.[9] introduced robust optimization to handle uncertain demand, but their model remains limited by its inability to address the spatial complexity of collaborative multi-UAV site selection in unstructured terrains.

Similarly, infrastructure inspection research, such as the work by Zheng et al.[11], employs multi-objective models to minimize operational costs. Yet, these approaches are specifically engineered for linear "line-of-sight" inspection (e.g., power grids), making them insufficiently adaptable to the expansive area coverage requirements of forest environments. Furthermore, siting models for road and urban traffic concentrate on traffic density[14], regional risk[17], and flight safety. A critical commonality among these studies is their reliance on simplified two-dimensional (2D) or network-constrained models, which fail to account for the three-dimensional (3D) topographical and environmental challenges inherent in forested regions.

To provide a systematic analysis of these methodological differences, Table 1 compares existing research with the proposed approach across five key dimensions.

**Table 1 Comparison of existing research methods in UAV hangar siting**

| Research scenario | Objective function | Key constraint | Algorithm | Indicators & limitations |
|---|---|---|---|---|
| Material logistics[7-9] | Minimize economic cost; minimize delivery time | UAV range; payload capacity; battery limits | Single-objective optimization; greedy; heuristics | Focused on distribution efficiency; neglects synergistic coverage between hangars |
| Infrastructure inspection[10-13] | Maximize inspection efficiency; minimize system cost | Linear network constraints; power availability | Task allocation; deep learning; Weighted-sum GA | Optimized for structured linear paths; low adaptability to non-linear forest area coverage |
| Road & traffic monitoring[14-17] | Maximize safety; minimize regional risk | Traffic density; street-level risk; 2D obstacles | Distributed siting; decentralized navigation | Relies on simplified 2D or network-constrained models; fails to address complex 3D terrain |
| Proposed method | Minimize construction cost and maximize area coverage | 3D topographical occlusion; redundancy; UAV power limits | NSGA-Ⅱ with MCDA preliminary screening | Pareto efficiency; system resilience; terrain-aware performance |

This systematic comparison underscores a significant research gap: Existing frameworks are predominantly tailored for structured environments and fail to address requirements unique to forest inspection, such as optimizing for synergistic area coverage and accounting for complex topographical occlusion. Forest area inspection presents unique challenges; ridge blockage, topographical undulation, and dense vegetation accelerate UAV performance degradation and complicate equipment maintenance. These constraints drastically alter both the set of feasible sites and the construction costs.

Unlike prior studies that focused on individual hangar indices, this paper emphasizes system-level efficiency through the synergistic deployment of multiple UAV hangars. The proposed methodology integrates a multi-criteria decision analysis (MCDA) for preliminary candidate screening with a multi-objective optimization model that enforces constraints for redundancy, endurance, and terrain-induced occlusion. Finally, the NSGA-Ⅱ is employed to find optimal solutions that balance cost and coverage efficiency[18].

The rest of this paper is structured as follows. Section 1 provides a systematic description of the multi-UAV hangar selection problem in forest areas. Section 2 proposes a preliminary screening method of hangar candidates based on MCDA, followed by the establishment of an optimization model for collaborative multi-UAV hangar selection in forest areas and the design of NSGA-Ⅱ algorithm for solving the model. Section 3 chooses a real forest area case for solving the problem and verifies the validity of the proposed method. Section 4 summarizes the study.

# 1 Problem Description

In multi-UAV forest inspection, hangars serve as critical energy replenishment and data interaction hubs, supporting all-weather, long-endurance missions. Their spatial topology fundamentally determines the swarm's operational radius and response timeliness. However, the unstructured forest environment imposes severe multi-dimensional challenges.

As illustrated in Fig.1, dramatic topographical undulations, such as ridges and valleys, induce nonlinear growth in UAV energy consumption and cause line-of-sight (LOS) occlusion, rendering traditional 2D Euclidean coverage models inadequate. And stringent ecological policies, limited road accessibility, and power requirements result in highly discretized and fragmented feasible domains for hangar construction.

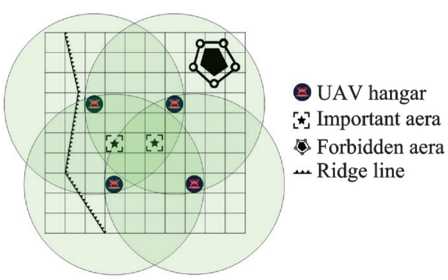


Fig.1 Schematic diagram of hangar selection for forest inspection

Furthermore, mission requirements exhibit spatial heterogeneity. High-risk priority zones demand redundant coverage from multiple hangars to ensure system resilience against single-point failures. Hangar siting is essentially a multi-dimensional Pareto game between coverage completeness, operational reliability, and construction costs, where simplified geometric models fail to capture complex constraints.

Consequently, this study addresses the challenge of identifying an optimal hangar configuration from a limited candidate set to balance coverage, efficiency, and cost. Characterized by mutually conflicting objectives and non-linear coupled constraints, this problem is a typical NP-hard challenge, necessitating advanced multi-objective evolutionary algorithms. This research establishes a robust spatial network foundation for subsequent collaborative path planning.

# 2 Methodology

This paper addresses the impact of topography on the construction of hangars and UAV performance in forest scenarios. First, geographic information for the target area is collected, including the digital elevation model (DEM), year-round meteorological data, power supply, and signal coverage. The region is processed using convex hull and grid-based methods. Based on this data, a MCDA scoring method is designed to select suitable candidate hangars locations. The focus then shifts to the collaborative capability of multiple hangars, considering the rationality and stability of their layout. A multi-objective optimization model for hangar selection is then developed. Finally, considering the characteristics of the model, a NSGA-Ⅱ algorithm is applied to solve the optimization problem and determine the final locations for hangar construction.

## 2.1 Multi-criteria decision-based candidate hangar selection

To improve the efficiency and accuracy of site selection, this paper follows UAV hangar selection guidelines. Hangar selection involves multiple criteria, including rigid criteria (e.g. prohibited areas and areas without power coverage) and flexible criteria (e.g. altitude and wind speed within predefined ranges). Due to the complexity of these criteria and the trade-offs between them, a single decision-making method is insufficient to consider all factors comprehensively. Therefore, a MCDA scoring method is adopted for the site selection decision.

MCDA is a systematic approach capable of handling complex decision problems with multiple evaluation criteria. In the case of UAV hangar selection, different criteria may conflict with one another. The MCDA method helps find the optimal tradeoff by evaluating the relative importance and constraints of each criterion. Specifically, the forest topographical data is first rasterized, and a scoring method is designed to evaluate each candidate location. Each candidate is assigned a composite score based on its compliance with rigid criteria and its performance within the range of flexible criteria. The optimal candidate locations are then selected. This approach enables the optimization of hangar selection under multidimensional constraints and requirements, improving the efficiency and reliability of subsequent inspection tasks.

UAV hangar siting must balance terrain suitability, infrastructure access and safety requirements. We first gather DEM, weather records, power-supply maps and forbidden-zone boundaries. Outliers and missing data are addressed using bilinear interpolation, and the data (elevation, slope, wind speed) are rasterized to a consistent spatial resolution to enable effective spatial analysis and overlay.

In the candidate-screening workflow, these criteria are systematically evaluated through two sequential stages. First, rigid constraints, absence of power supply or presence within prohibited zones, are applied as binary filters to remove unsuitable raster cells. This filtering step yields a set of technically feasible cells. Second, the remaining feasible cells are scored based on flexible criteria using weights derived from an analytic hierarchy process (AHP). Three domain experts, a forest-management officer, UAV-maintenance engineer, and remote-sensing specialist, independently complete pairwise comparisons among the three criteria, and their evaluations are aggregated via the geometric-mean method. The principal eigenvector method provided normalized weights: 0.40 (elevation), 0.35 (slope), and 0.25 (wind), with a consistency ratio of 0.06, within the acceptable threshold (0.10).

The selection process is implemented using a scoring system, with detailed criteria based on compliance with each factor. The pseudocode for this process is as follows.

Algorithm: Multi-criteria drone hangar selection (MCDHSS)

Input: CandidatePoints, DEM, WindMap, PowerMap, Forbidden masks, AHP weights $w=\{w_1, w_2, w_3\}$

Output: SelectedPoints //top-ranked feasible sites

(1) Feasible $\leftarrow \{p \in$ CandidatePoints$|$
PowerMask $(p)=1 \wedge$ ForbiddenMask$(p)=0\}$// hard-constraint filtering

(2) for each $p \in$ Feasible do
score$(p) \leftarrow w_1 \cdot$Elev$(p) + w_2 \cdot$Slope$(p) + w_3 \cdot$Wind$(p)$//flexible-criteria scoring
end for

(3) SelectedPoints $\leftarrow$ top $N$ points ranked by score$(p)$

(4) return SelectedPoints //Sort and return top $N$ candidates

## 2.2 Multi-objective hangar selection model

### 2.2.1 Model assumptions and definitions

The model is based on the following assumptions.

(1) Each UAV is equipped with a rotary camera, enabling comprehensive monitoring of the target area while maintaining a fixed hovering position.

(2) Each UAV hangar has a fixed-radius circular coverage area centered at the hangar.

(3) During task execution, the UAV can maintain a stable communication link with the control center to ensure real-time data transmission.

(4) The task area is divided into common and important zones, where the important zone requires coverage by at least two hangars.

(5) The terrain consists of suitable and forbidden construction areas.

The fixed-radius coverage and uniform UAV performance assumed in this study are theoretical simplifications for the initial planning stage, which help reduce computational complexity. In practice, these assumptions should be validated under real environmental conditions. In forest environments, the effective service radius may vary due to dynamic factors such as wind speed and canopy density. To account for this, the service radius can be extended to a time-dependent function $r(t)$. For example

$$r(t)=r_0\cdot(1-\alpha W(t)-\beta C(t)) \tag{1}$$

where $W(t)$ denotes the wind speed at time $t$; $C(t)$ is the canopy density; and $\alpha$ and $\beta$ are the sensitivity coefficients reflecting environmental impact.

From an algorithmic perspective, such dynamic information can be incorporated using a rolling-horizon strategy, where model parameters are periodically updated based on real-time or seasonal data. This extension will be explored in future work.

### 2.2.2 Symbol definitions

To facilitate reading, all the symbols used in this paper are introduced in Table 2.

**Table 2 Symbol descriptions**

| Notations | Description |
|---|---|
| $x_i$ | Usage of candidate hangar $i$, where 1 indicates selection, and 0 indicates non-selection |
| $G$ | Set of topographical grids, divided into $m$ rows and $n$ columns |
| $C$ | Set of candidate hangars after preliminary screening |
| $L$ | Set of points representing main topographical lines |
| $r$ | Effective coverage radius of a UAV hangar |
| $d_{\max}$ | Maximum ideal flight range of the selected UAV |
| $O_{ij}/O_{\max}$ | Overlap rate between candidate hangars $i$ and $j$, and the maximum allowed overlap rate |
| $C_k$ | Area coverage of the region by candidate hangar $k$ |
| $D_k$ | Coverage matrix of candidate hangar $k$ |
| $B_k/B_{\max}$ | Proportion of area blocked by topographical lines for candidate hangar, and the maximum allowed blocked area proportion |
| $E_k/E_{\min}$ | Proportion of effective area for candidate hangar, and the minimum allowed effective area proportion |

### 2.2.3 Model objectives and constraints

Traditional multi-objective site-selection problems, such as city-wide Wi-Fi or urban depot planning, assume a structured environment and 2D obstacles (roads, buildings). Forest inspection is different. It must handle rugged terrain, dense canopy cover and legally protected no-fly areas. These natural and regulatory constraints drastically alter both the set of feasible sites and the applicable model constraints. Accordingly, our model embeds four forest-specific constraints, including terrain-induced occlusion, ecological no-fly zones, redundant coverage of critical areas and, planned for future work, dynamic environmental updates. Their mathematical realizations are presented below together with the standard coverage and cost objectives.

Practical applications show that a simplified fixed-radius model[19] can meet coverage needs in most scenarios while reducing computational complexity. Therefore, in this study, the coverage area of each hangar is defined as a fixed-radius circle. The hangar selection problem in forest areas is modeled as a multi-circle placement optimization problem. In this problem, each circle represents the coverage area of a hangar, and the center of each circle corresponds to the location of the hangar. This approach allows for the effective evaluation and optimization of hangar layouts, aiming to achieve comprehensive coverage of the forest area. The problem is formally described as

$$F_1=\min\sum_{i=1}^{s}x_i \tag{2}$$

$$F_2=\max\bigcup_{i=1}^{s}C_i x_i \tag{3}$$

where the objective of $F_1$ is to minimize hangar construction costs by reducing the number of sites; the objective of $F_2$ is to maximize the total coverage area of the sites; $\sum_{i=1}^{s}x_i$ represents the total number of hangars constructed; and $\bigcup_{i=1}^{s}C_i x_i$ denotes the total coverage area of the hangars.

The hangars must satisfy several constraints, including overlap rate, significant topographical obstruction, effective coverage area, system redundancy, emergency return capabilities, and high coverage of important areas. The constraints of the model are set as

$$O_{ij}\cdot x_i\cdot x_j\leqslant O_{\max}\quad \forall i,j\in C,i\neq j \tag{4}$$

$$B_k\cdot x_k\leqslant B_{\max}\quad \forall k\in C \tag{5}$$

$$E_k\cdot x_k\geqslant E_{\min}\quad \forall k\in C \tag{6}$$

$$\sum_{j\in C,j\neq k} x_j \cdot I\{d(x_k,x_j)\leqslant 2r\}\geqslant 1$$
$$\forall k\in\{i|x_i=1\} \tag{7}$$

$$\sum_{k=1}^{n} x_k \cdot I\{d(x_k,p)\leqslant \eta d_{\max}\}\geqslant 1 \quad \forall p\in P \tag{8}$$

$$\sum_{k=1}^{n} x_k \cdot I\{d(x_k,p)\leqslant r\}\geqslant 2 \quad \forall p\in P^* \tag{9}$$

For every pair of candidate hangars, we measure the distance between their centers. If this distance is at least twice the service radius, the two coverage circles do not overlap and the pair passes the test automatically. If the circles do intersect, we calculate the area of their overlap ratio (analytically or by counting raster cells) and express it as a fraction of one full coverage circle. Eq.(4) ensures that the overlap rate between any two selected hangars does not exceed a specified threshold. For every candidate hangar we discretize its theoretical service disk into a uniform planar grid. We trace the straight line that connects the hangar center to each grid-cell center, sampling the DEM at fixed spatial intervals along this line. At each sampling point we compare the ground elevation with the height of the line of sight. If the ground height exceeds the line-of-sight height, the target cell is classified as occluded. After evaluating all cells, the occlusion ratio is calculated as the proportion of cells classified as occluded. Hangars whose occlusion ratios exceed the prescribed threshold are excluded from further optimization. Eq.(5) ensures that the proportion of the area obstructed by significant topographical (such as major ridgelines) for any selected hangar is less than a specified threshold. For each candidate hangar, the effective coverage ratio is calculated by dividing the area of the inspection domain within the hangar's service circle by the total area of that circle. Eq.(6) ensures that for candidate hangar is greater than a specified threshold. Eq.(7) defines the redundancy constraint: The coverage area of each selected hangar must overlap with the coverage area of at least one other selected hangar. This ensures system resilience by allowing adjacent hangars to provide backup coverage in case of a single hangar failure. Eq.(8) defines the emergency return constraint: When a UAV departs from any point in the topography, it must be able to return to a hangar within its maximum flight range. Here, $d_{\max}$ represents the UAV's maximum flight range, and $I\{\ \}$ is an indicator function, where if the UAV can return to the hangar, $I\{\ \}=1$, otherwise $I\{\ \}=0$. $p$ refers to any region in the topography. Eq.(9) ensures that critical task areas are covered by at least two hangars, which enhances the completion rate of critical tasks. Here, if the point $x_k$ is within the coverage of the hangar, $I\{\ \}=1$, otherwise $I\{\ \}=0$. $p$ refers to the critical task area in the topography.

This model, by setting multi-objective optimization goals and multiple constraints, quantifies the various requirements for hangar selection, providing comprehensive decision support for the UAV hangar selection in inspection tasks.

### 2.3 Model solving based on NSGA-Ⅱ algorithm

This multi-objective model involves conflicting objectives that balance deployment cost, inspection coverage, and nonlinear constraints. This complexity makes traditional mathematical methods insufficient. In contrast, heuristic evolutionary algorithms have shown significant advantages in multi-objective optimization problems. Multi-objective evolutionary algorithms (MOEAs)[20] use a probabilistic search strategy, offering strong adaptability and stability, meaning that even poor individual solutions do not significantly affect the overall performance of the system. NSGA-Ⅱ, as a classic MOEA, is widely used for multi-objective optimization due to its rapid convergence, low computational complexity, and strong diversity solution.

Previous research shows that genetic algorithms are effective for multi-objective site selection problems. Therefore, this paper uses the NSGA-Ⅱ with elitist strategies to solve the model. NSGA-Ⅱ enhances global optimization capabilities through non-dominated sorting, crowding distance calculation, and elitism retention. Non-dominated sorting ranks solutions based on dominance relationships. This ensures that the first-rank Pareto-optimal set contains well-balanced solutions. The crowding distance measures the sparsity of solutions in the objective space, maintaining an even distribution of solutions on the Pareto front and avoiding local optima.

The elitist retention mechanism further improves the algorithm's convergence, allowing non-dominated solutions to be directly passed to the next generation, thereby enhancing the quality and diversity of the final solution set.

To solve the multi-objective optimization model, this paper designs a NSGA-Ⅱ algorithm. The steps of the algorithm are outlined below.

First, the population is initialized using binary encoding to represent the selection status of each candidate hangar. Each hangar selection scheme corresponds to an individual in the population, and the gene values of the individual's chromosome corresponds to the status of the candidate hangars. The chromosome length is set to the number of candidate hangars, denoted as $M_{\text{cand}}$. The chromosome genotype $X_k=(x_1,x_2,\cdots,x_{M_{\text{cand}}})$, where $x_i=1$ if the $i$th candidate hangar is selected, and $x_i=0$ if it is not selected. The population size is $M$ and it is initialized randomly with each individual representing a hangar selection scheme. For example, Table 3 shows the genotype of an individual, where only candidate hangar 2 is selected for construction among candidates 1—4.

**Table 3 Binary encoding**

| Gene position | 1 | 2 | 3 | 4 | ⋯ | $M_{\text{cand}}-1$ | $M_{\text{cand}}$ |
|---|---|---|---|---|---|---|---|
| Gene value | 0 | 1 | 0 | 0 | ⋯ | 0 | 1 |

Next, the fitness of the individuals in the population is evaluated. This paper uses two objective functions as fitness evaluation indicators: (1) Maximizing the number of covered terrain points, i. e., maximizing coverage; (2) minimizing the number of selected hangars, i. e. minimizing the number of hangars. These two objective functions are used to comprehensively evaluate hangar selection schemes.

$$f_1=\frac{\bigcup_{i=1}^{s} C_i x_i}{C_{\text{need}}} \tag{10}$$

$$f_2=\sum_{i=1}^{s} x_i \tag{11}$$

The quality of the selection scheme is assessed through these two functions. A higher value of $f_1$ and a lower value of $f_2$ indicate a better solution.

Individuals are selected through non-dominated sorting and crowding distance. Based on the individuals' fitness, the Pareto optimal solutions are prioritized, and the crowding distance for each individual in each non-dominated layer is calculated to retain more diverse solutions. Evolution is then performed on the filtered population. Individuals undergo two-point crossover (Xovdp), where two crossover points are randomly selected from the parent chromosomes, and the genetic material between the points is exchanged to generate new offspring. After crossover, binary mutation (Mutbin) is applied, where one or more positions in the individual's chromosome are randomly selected and mutated, changing gene 0 to 1 or gene 1 to 0. After evolution, the population is updated using the elitist tournament selection method (etour), ensuring that the optimal solutions are not discarded.

The NSGA-Ⅱ algorithm in this paper adopts two stopping criteria:

(1) The algorithm terminates when the maximum number of iterations is reached.

(2) The algorithm terminates when the Pareto optimal solution set no longer significantly changes over several consecutive generations.

The final output is the Pareto optimal solution set, which provides the decision-makers with a selection of optimal schemes. The pseudocode for the NSGA-Ⅱ algorithm is as follows.

Algorithm: Collaborative multi-UAV hangar selection with NSGA-Ⅱ (CMU-NⅡ)

Input: TerrainData, CandidatePoints, NSGA Ⅱ_Params, Maximum Generations ($T$)

Output: Pareto optimal solution set (ParetoFront)

(1) Initialize population $P$

(2) Define fitness function Fitness($P$) and constraint violation function ConstraintViolation($P$)

(3) Set $t=0$ //Main loop

(4) while $t<T$ do //Fitness evaluation

(5) EvaluateFitness($P$)

(6) for each individual $p$ in $P$ do

(7) Calculate coverage score $f_1(p)$ and cost score $f_2(p)$

(8) Calculate constraint violation of $p$ using ConstraintViolation($p$)

(9) end for

```
end Procedure
P_non_dominated ← NonDominatedSorting(P)
CalculateCrowdingDistance (P_non_dominated)
Offspring ← Crossover(P_non_dominated)
UnionPopulation ← P∪Mutate (Offspring)
//Elite strategy for population selection
EvaluateFitness(UnionPopulation)
P←EliteSelection(UnionPopulation, NSGAⅡ_Params.M)
UpdateParetoFront (P, ParetoFront) // Update Pareto optimal solution set
t ← t + 1
if ConvergenceCriteriaMet (ParetoFront, NSGAⅡ_Params) or t >= T then
    break
end if
end while
Return ParetoFront
```

Let $T$ denote the number of generations, $P$ the population size, $N_{\text{grid}}$ the number of terrain grid cells, $M_{\text{cand}}$ the number of candidate hangar sites (chromosome length), and $k$ ($k \ll M_{\text{cand}}$) the average number of hangars selected in a chromosome. The dominant task of each generation is merging $k$ coverage masks over $M_{\text{cand}}$ cells for all $P$ individuals, so the total running time is

$$T = O(\text{TP}N_{\text{grid}}k)\ (\text{worst case } k = M_{\text{cand}}) \tag{12}$$

## 3 Application and Results

This section introduces the real terrain data used for the study and defines the parameters for the NSGA-Ⅱ algorithm based on the operational conditions of the UAV hangars. Using the established model and algorithm parameters, the NSGA-Ⅱ algorithm is employed to solve the optimization problem. The results are then compared with those obtained from other algorithms to validate the effectiveness of the proposed method. Finally, the results are analyzed and discussed.

### 3.1 Case description

The study is conducted in a forest region in Nanjing, China. The area is characterized by significant environmental and population sensitivity due to the presence of schools, residential zones, and a reservoir, which are defined as critical areas for the siting model.

The study utilized topographical data from NASA's Shuttle Radar Topography Mission (SRTM) to generate a DEM with a 30 m spatial resolution (ID: SRTM1N31E118V3), as visualized in Fig.2. The raw data was projected to the WGS84 UTM coordinate system for geographic accuracy. Pre-processing steps included void filling, smoothing, and the calculation of slope and aspect using geographic information system (GIS) tools to enhance data quality. The irregular study area boundary, extracted from OpenStreetMap, was converted into a convex hull to define a regular experimental area (Fig.3). Finally, this area was discretized into a uniform grid with 100 m cells for analysis.

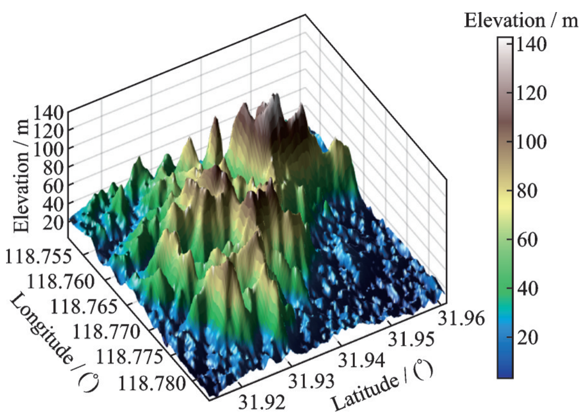


Fig.2 Elevation model of research region (3D)

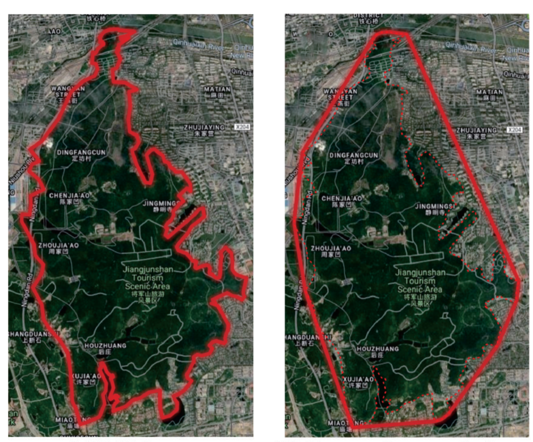

(a) Initial area (b) Processed convex hull area

Fig.3 Satellite images of the region

Spatial constraints were defined based on pre-identified critical zones, as shown in Fig.4. These included important areas (e.g. schools) requiring enhanced surveillance and forbidden areas (e.g. reservoirs), where hangar construction is prohibited. These zones provided explicit spatial constraints for the optimization algorithm.

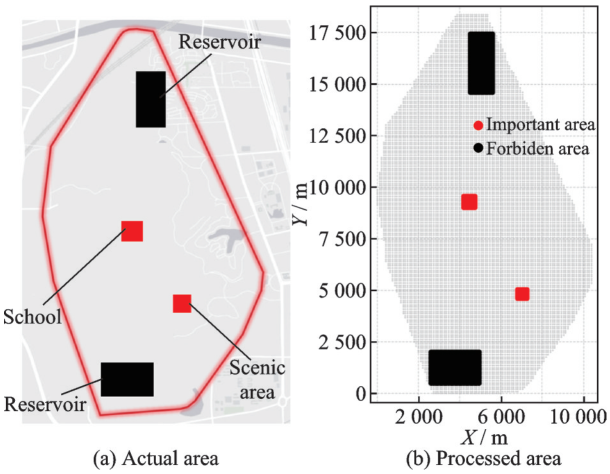


Fig.4 Schematic of critical areas and forbidden zones

The algorithm's parameter settings are as follows. The service radius of hangars is set to 3 000 m, with a grid edge length of 100 m. The minimum effective coverage rate and maximum terrain occlusion rate are set to 0.4 and 0.5, respectively, to meet coverage requirements and topographical constraints. The maximum overlap rate is set to 0.7 to optimize resource utilization. The crossover and mutation rates are set to 0.9 and 0.1, respectively, to maintain diversity in the search space. The population size is 100 individuals, with a maximum of 200 iterations, ensuring algorithm stability and convergence performance. The program is implemented in Python 3 and executes on an experimental simulation platform with the following specifications: Windows 10 operating system, 13th Gen Intel (R) Core (TM) i9-13900K processor at 3.00 GHz, and 128 GB of memory.

## 3.2 Optimization results

### 3.2.1 Preliminary selection of candidate hangars

Following the preliminary screening process, Fig.5 illustrates the resulting UAV hangar selection, where 160 candidate sites meeting the rigorous selection criteria were identified using GIS data. The spatial distribution of these points systematically adheres to the site selection specifications by avoiding forbidden zones and maintaining appropriate operational intervals. However, a detailed spatial analysis reveals that this distribution is non-uniform across the research region. Specifically, as visualized in Fig.5, candidate points are significantly sparser in the lower-left and upper-right quadrants. This observed sparsity is highly consistent with the spatial constraints defined in Fig.4, where these specific regions contain the highest density of forbidden zones, such as the reservoir and residential areas, combined with lower elevation profiles that are fundamentally unsuitable for hangar construction.

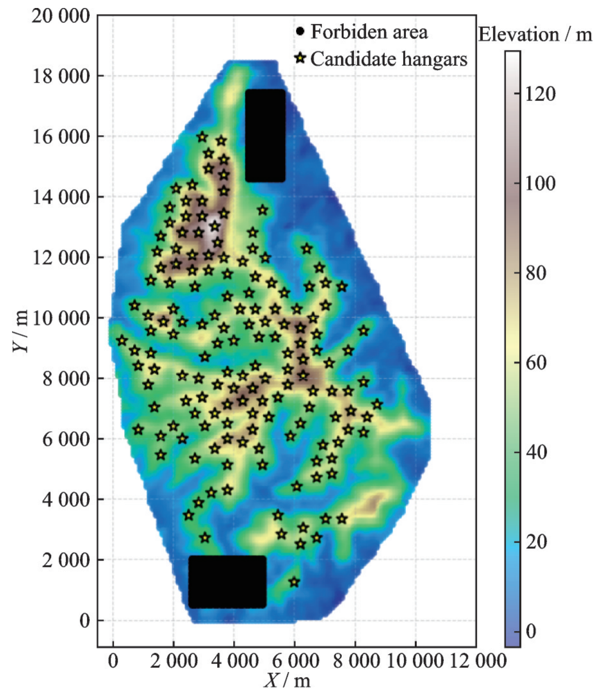


Fig.5 Candidate hangar results

The strategic layout of these candidate points ensures effective coverage and operational reliability for UAV inspections in mountainous areas, while adhering to topographical constraints and regulatory requirements. This approach demonstrates comprehensive consideration of geographical, technical, and regulatory parameters in UAV site selection.

### 3.2.2 Analysis of terrain occlusion on coverage

To demonstrate the necessity of a terrain-aware siting model, we analyzed the impact of topographical features on a hangar's effective coverage. Fig.6 presents a compelling example using candidate point No.80, which is situated near a major ridgeline.

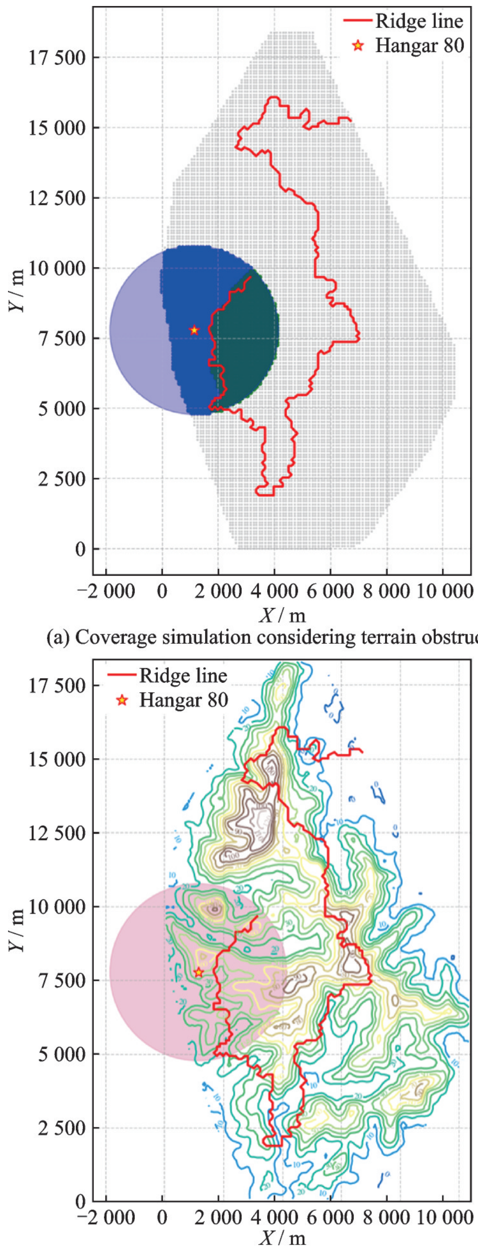


(a) Coverage simulation considering terrain obstruction

(b) Coverage simulation in contour map

Fig.6 Coverage simulation results for candidate point 80

The analysis reveals that the hangar's theoretical circular service area is severely fragmented by the terrain. A significant portion of the coverage is classified as an occluded region (green area), where line-of-sight is blocked by the ridgeline. Missions within this zone would incur substantially higher operational costs and signal loss risks compared to the unobstructed zone (blue area). This fragmentation drastically reduces the site's practical value and efficiency.

This single case starkly illustrates that a simplistic fixed-radius assumption is inadequate for complex forest environments. It underscores the critical importance of integrating topographical occlusion into the selection process, which is a core strength of our proposed multi-objective optimization model.

### 3.2.3 Multi-objective optimal deployment solutions

The NSGA-Ⅱ was employed to solve the multi-objective optimization model, generating a set of Pareto optimal solutions[21] that balance deployment cost (number of hangars) and inspection coverage. These solutions provide decision-makers with a range of optimized trade-offs.

As illustrated in Fig.7, the Pareto front clearly reveals the relationship between the two competing objectives. A sharp increase in coverage is observed when the number of hangars grows from four to eight. However, beyond this point, the curve flattens, indicating diminishing returns: Deploying additional hangars yields only marginal gains in coverage at a significantly higher cost. This insight is crucial to resource allocation, allowing decision-makers to identify a "sweet spot" that balances cost and effectiveness.

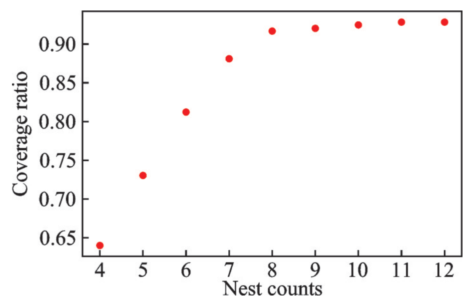


Fig.7 Pareto front

To demonstrate the practical viability and spatial intelligence of the proposed solutions, we selected a representative balanced solution, Individual 23, which deploys 11 hangars to achieve 92.7% coverage, Fig.8 visualizes the overall deployment layout in relation to the terrain. The selected hangars are strategically distributed across the area, effectively avoiding major topographical obstructions and forming a collaborative coverage network. Furthermore, it highlights the solution's adherence to critical mission constraints. Both designated important areas are covered by at least two hangars, satisfying the dual-coverage requirement and ensuring enhanced reliability for monitoring sensitive zones.

The layout successfully avoids the forbidden areas, showcasing the model's ability to integrate complex spatial constraints. This configuration not only optimizes resource allocation but also enhances the resilience of the inspection system against single-point failures, providing a robust and efficient deployment scheme for real-world application.

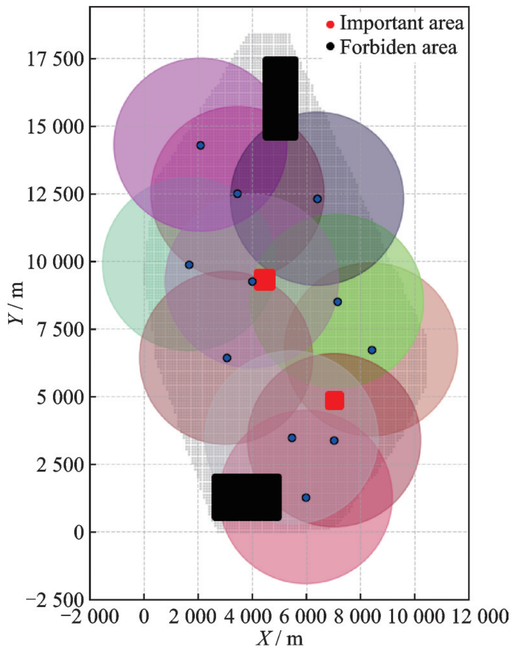


Fig.8 Coverage of important areas in scheme 23

### 3.3 Analysis and validation

#### 3.3.1 Algorithm performance analysis

To validate the performance of the proposed NSGA-Ⅱ algorithm, we evaluated its convergence, solution quality, and computational efficiency. The algorithm's convergence behavior and the quality of the resulting solution set were assessed using two standard metrics: Hypervolume (HV) and Spacing. HV measures the coverage and diversity of the solution set, with higher values indicating better performance. Spacing measures the uniformity of the solution distribution along the Pareto front, where smaller values signify a more even distribution.

Fig.9 plots the evolution of both metrics over 200 generations. The HV value exhibits rapid growth in the initial phase and stabilizes around the 40th generation. This indicates that the algorithm converges quickly, efficiently identifying a high-quality and diverse set of solutions early in the optimization process. Concurrently, the Spacing value starts high, reflecting an initially uneven distribution of solutions, and then progressively decreases, converging to a small, stable value. This demonstrates that the algorithm successfully refines the solution set to achieve a uniform distribution across the objective space.

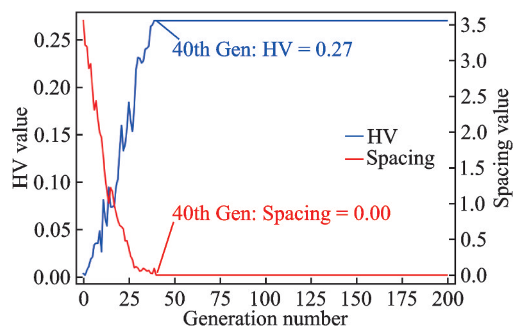


Fig.9 HV and Spacing iteration plot

Together, these results confirm that the algorithm not only converges efficiently but also maintains a well-distributed and high-quality Pareto front, ensuring robust and reliable final solutions.

The computational performance was analyzed to ensure the method's practicality for real-world applications. Fig.10 illustrates the runtime behavior of the NSGA-Ⅱ algorithm. The per-generation run-

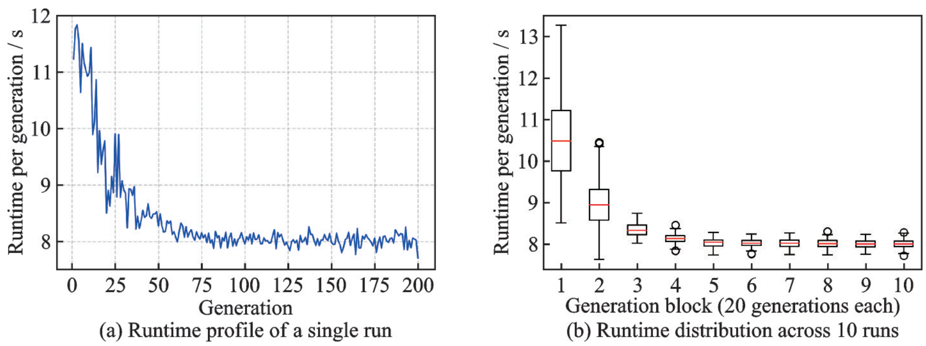


Fig.10 Runtime analysis of NSGA-Ⅱ

time decreases sharply during an initial warm-up phase (first 10 generations) before stabilizing at approximately 8 s per generation for the remainder of the run. Box plots from ten independent runs confirm that this runtime profile is highly consistent and repeatable, with minimal variation.

To assess scalability, the algorithm was tested on problems of increasing size, as detailed in Table 4. The results demonstrate that the computational effort scales linearly with the product of the number of grid cells ($N_{grid}$) and candidate sites ($M_{cand}$). For instance, quadrupling the problem scale resulted in an approximately four-fold increase in total runtime. Even the largest tested instance was solved within an acceptable time frame on a standard workstation, demonstrating that the proposed method is computationally feasible and scalable for substantially larger and more complex deployment scenarios.

**Table 4 Runtime proportionality to grid-candidate scale**

| Scale factor | $N_{grid}$ | $M_{cand}$ | Total runtime/s | (Avg runtime/generation)/s |
|---|---|---|---|---|
| Baseline | 12 000 | 100 | 978 | 4.89 |
| Medium | 24 000 | 200 | 1 932 | 9.66 |
| Large | 48 000 | 400 | 4 013 | 20.07 |

### 3.3.2 Comparative analysis with benchmark algorithms

To validate the effectiveness of the proposed approach, its performance was benchmarked against three other algorithms: A greedy heuristic (Greedy), a single-objective genetic algorithm (GA) using weighted summation, and another well-regarded multi-objective method, MOEA/D. To ensure the validity of the comparative analysis, all evolutionary algorithms shared the same population size (100) and termination criteria (200 generations). Specifically, the single-objective GA utilized a weighted sum fitness function to aggregate the competing objectives of coverage and construction cost. Following normalization of the objective values, weights were set as $w_{coverage}=0.5$ and $w_{cost}=0.5$ to normalized coverage and cost. MOEA/D was implemented using the Chebycheff decomposition with a neighborhood size of 20. The Greedy algorithm followed a maximal incremental coverage strategy, selecting the site with the highest marginal gain at each step until 12 hangars were deployed.

The core performance metrics, summarized in Table 5, reveal the superior balance achieved by the NSGA-Ⅱ algorithm. It secured 92.75% coverage with only 11 hangars and converged in just 40 generations. In contrast, the Greedy algorithm required 12 hangars for similar coverage, indicating lower resource efficiency. Although MOEA/D matched the solution quality of NSGA-Ⅱ, its computational cost was significantly higher, with a 50% longer runtime and a much slower convergence of 180 generations. The single-objective GA performed suboptimally across all metrics.

**Table 5 Algorithm comparison**

| Algorithm | NSGA-Ⅱ | GA | MOEA/D | Greedy |
|---|---|---|---|---|
| Number of hangars | 11 | 11 | 11 | 12 |
| Coverage rate/% | 92.75 | 88.39 | 92.75 | 92.86 |
| Convergence generation | 40 | 190 | 180 | 1 |
| Runtime/s | 1 478 | 1 985 | 2 245 | 978 |

To provide a deeper, multi-dimensional evaluation, we introduced two advanced assessment metrics. First, the facility to coverage efficiency ratio (FCER) was used to measure cost-effectiveness, with higher values indicating better performance. As shown in Fig.11, the solutions generated by NSGA-Ⅱ consistently dominate the top ranks, confirming its superior ability to produce the most economical configurations.

Second, the technique for order preference by similarity to ideal solution (TOPSIS) method was employed to provide a holistic ranking of all solutions based on their proximity to a theoretical "ideal solution". The results, visualized in Fig.12, are unequivocal: NSGA-Ⅱ solutions consistently occupy the highest ranks and cluster nearest to the ideal point, demonstrating a robust ability to optimally balance high coverage with low construction cost. In contrast, the solutions from other algorithms are dispersed across lower ranks, confirming they fail to achieve a satisfactory trade-off.

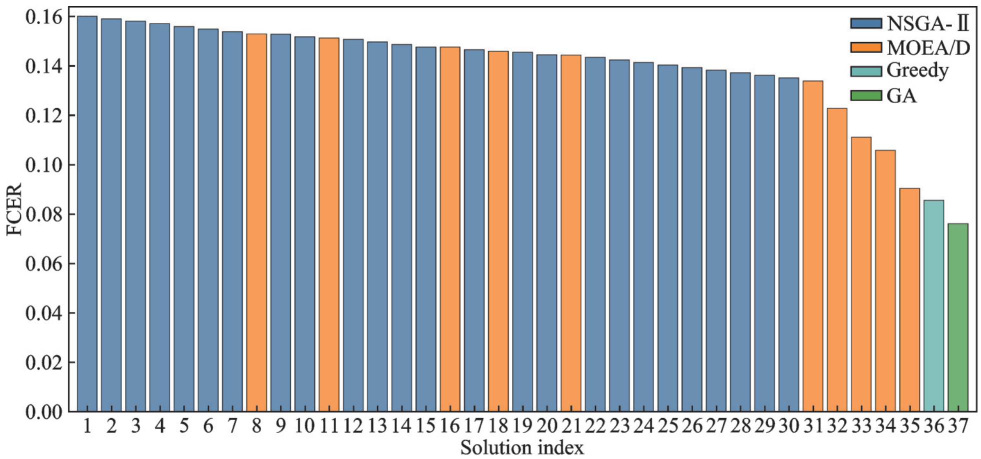


Fig.11 FCER of different algorithm

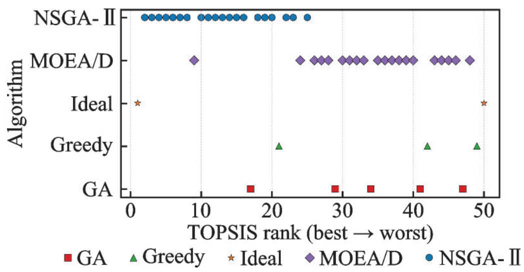


Fig.12 Algorithm ranking

In summary, the comprehensive comparative analysis from three distinct perspectives, core metrics, cost-effectiveness, and holistic ranking, collectively substantiates the superiority and robustness of the proposed NSGA-Ⅱ approach for solving the complex UAV hangar deployment problem in challenging terrains.

### 3.3.3 Parameter sensitivity analysis

To validate the robustness of the NSGA-Ⅱ algorithm performance and optimize parameter settings, we conducted a sensitivity analysis on the key genetic parameters, namely crossover and mutation rates. The crossover rate was systematically varied across the values [0.1, 0.3, 0.5, 0.7, 0.9], and the mutation rate across [0.01, 0.05, 0.1, 0.2]. Algorithm performance was evaluated by observing the convergence speed, measured by the number of generations required for stabilizing fitness values.

As we can see in Fig.13, lower crossover rates (e.g., 0.1 and 0.3) lead to significantly slower convergence, typically requiring around 160—180 generations to reach stability. Conversely, a higher crossover rate (0.9) provides the fastest convergence, stabilizing around the 100th generation. Similarly, mutation rates at the extremes (0.01 and 0.2) negatively impacts convergence speed, with optimal performance observed at a mutation rate of 0.1, requiring approximately 110 generations for convergence. Consequently, the crossover rate and mutation rate are set to 0.9 and 0.1, respectively, to effectively maintain diversity in the search space and enhance computational efficiency.

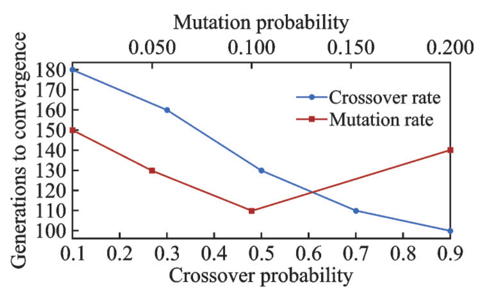


Fig.13 Sensitivity of NSGA-Ⅱ convergence to crossover and mutation probabilities

## 4 Conclusions

We present a multi-objective optimization model to minimize construction costs and maximize the total coverage rate of UAV hangars. This model addresses unique challenges posed by complex terrain in forested areas. The model incorporates key constraints, such as effective coverage, UAV power limits, and anti-interference, and effectively evaluates the advantages and disadvantages of site configurations while optimizing hangar layouts to enhance inspection efficiency and system reliability. The NSGA-Ⅱ algorithm demonstrates advantages in fast convergence and solution diversity. Simulation and comparison results show that NSGA-Ⅱ effectively balances coverage and the number of hangars, achieving 92.7% coverage with only 11 hangars, significantly outperforming MOEA/D, the greedy algorithm and the single-objective genetic algorithm. Additionally, the algorithm provides a rich set of Pareto solutions, offering flexibility for decision-makers to trade off between various costs and coverage requirements. The results provide valuable decision support for the efficient deployment of UAV inspection systems in forest areas, balancing coverage needs, economic factors, and cost reduction.

The current framework already honors ecological and regulatory limits by excluding statutory no-fly zones and requiring dual coverage of sensitive habitats, thereby improving both safety and legal compliance. To strengthen its real-world utility, future work will add road-network accessibility layers and season-dependent ecological or administrative constraints, ensuring that recommended sites remain serviceable as external conditions change. We will also link the static siting module to dynamic schedulers for task assignment, energy-aware routing, and multi-UAV coordination. Flight tests at representative forest sites will record tracks and power logs to verify the fixed-radius assumption; if deviations emerge, we will recalibrate it and derive adjustment rules tailored to each aircraft type and weather condition. These data-driven refinements will prepare the model for operational deployment and move it toward a fully automated, adaptive inspection system.

The results of this research are applicable not only to the selection of UAV hangar sites for forest inspections but also to the deployment of UAVs in other complex terrains. The planned extensions will contribute toward building a more intelligent, adaptive, and automated UAV inspection system for complex and dynamic environments.

## References

[1] DOORNBOS J, BENNIN K E, BABUR Ö, et al. Drone technologies: A tertiary systematic literature review on a decade of improvements[J]. IEEE Access, 2024, 12: 23220-23239.

[2] CUMMINGS M L, MITCHELL P J. Automated scheduling decision support for supervisory control of multiple UAVs[J]. Journal of Aerospace Computing, Information, and Communication, 2006, 3(6): 294-308.

[3] PU H, ZHEN Z, XIA M. Flight control system of unmanned aerial vehicle[J]. Transactions of Nanjing University of Aeronautics and Astronautics, 2015, 32(1): 1-8.

[4] HAI N D, DONG L K, MEN D T, et al. Spatiotemporal contribution of participants in patrolling efforts from a forest station, Puhu nature reserve, Vietnam[J]. Sustainability, 2021, 13(23): 13210.

[5] SOTILLE M E, BREMER U F, VIEIRA G, et al. Evaluation of UAV and satellite-derived NDVI to map maritime Antarctic vegetation[J]. Applied Geography, 2020, 125: 102322.

[6] TANG L N, SHAO G F. Drone remote sensing for forestry research and practices[J]. Journal of Forestry Research, 2015, 26(4): 791-797.

[7] WANG X Y, POIKONEN S, GOLDEN B. The vehicle routing problem with drones: Several worst-case results[J]. Optimization Letters, 2017, 11(4): 679-697.

[8] MURRAY C C, CHU A G. The flying sidekick traveling salesman problem: Optimization of drone-assisted parcel delivery[J]. Transportation Research Part C: Emerging Technologies, 2015, 54: 86-109.

[9] CHENG J H, ZHOU Y F, WU C Z, et al. Collaborative truck-drone-motorcycle delivery of emergency supplies for mountain wildfire suppression[J]. Computers & Industrial Engineering, 2024, 196: 110468.

[10] LUO Y H, YU X, YANG D S, et al. A survey of intelligent transmission line inspection based on unmanned aerial vehicle[J]. Artificial Intelligence Review, 2023, 56(1): 173-201.

[11] ZHENG H, WANG H X, ZHANG T P, et al. The collaborative power inspection task allocation method of "unmanned aerial vehicle and operating vehicle"[J]. IEEE Access, 2021, 9: 62926-62934.

[12] LI H, DONG Y Q, LIU Y X, et al. Design and implementation of UAVs for bird's nest inspection on transmission lines based on deep learning[J]. Drones, 2022, 6(9): 252.

[13] NGUYEN V S, NGUYEN T H. Energy outage analysis of aerial UAV-enabled SWIPT deployments[J]. IEEE Access, 2024, 12: 27147-27157.

[14] ZHONG Y C, YE S W, LIU Y Z, et al. A route planning method for UAV swarm inspection of roads fusing distributed droneport site selection[J]. Sensors, 2023, 23(20): 8479.

[15] LIU C F, WICKRAMASINGHE N D, SURAWEERA H A, et al. URLLC-aware proactive UAV placement in Internet of vehicles[J]. IEEE Transactions on Intelligent Transportation Systems, 2024, 25(8): 10446-

10451.

[16] HUANG H L, SAVKIN A V, HUANG C. Decentralized autonomous navigation of a UAV network for road traffic monitoring[J]. IEEE Transactions on Aerospace and Electronic Systems, 2021, 57(4): 2558-2564.

[17] CHEN H F, GAO X W, LI H H, et al. A framework for the optimal deployment of police drones based on street-level crime risk[J]. Applied Geography, 2024, 162: 103178.

[18] YIN P, MU L. Modular capacitated maximal covering location problem for the optimal siting of emergency vehicles[J]. Applied Geography, 2012, 34: 247-254.

[19] ERZIN A, LAGUTKINA N, IORAMISHVILI N. Barrier covering in 2D using mobile sensors with circular coverage areas[M]//Learning and Intelligent Optimization. Cham, Switzerland: Springer International Publishing, 2020: 342-354.

[20] SASAKI D, OBAYASHI S. Efficient search for trade-offs by adaptive range multi-objective genetic algorithms[J]. Journal of Aerospace Computing, Information, and Communication, 2005, 2(1): 44-64.

[21] IANCU D A, TRICHAKIS N. Pareto efficiency in robust optimization[J]. Management Science, 2013, 60(1): 130-147.

**Acknowledgements** This work was supported by the National Natural Science Foundation of China (No. 52172328), the National Key R&D Program of China (No. 2022YFB2602403), and Postgraduate Research & Practice Innovation Program of Jiangsu Province (No.KYCX24_0598).

**Authors**

**The first author** Mr. **QIAN Long** received his B.S. degree in transportation from Nanjing University of Aeronautics and Astronautics (NUAA) in 2023, where he is currently pursuing his M.S. degree. His research interests include UAV hangar siting and path planning.

**The corresponding authors** Mr. **LIU Jixin** received his master's degree from Nanjing Normal University in 1999. He is currently an associate professor of College of Civil Aviation, NUAA. He His research interests include human factors, aviation English, and air traffic management. Mr. **JIANG Hao** is currently pursuing his Ph.D. degree at Nanjing University of Aeronautics and Astronautics. His research interest is air traffic flow management.

**Author contributions** Mr. **QIAN Long** designed the study and wrote the manuscript. Prof. **LIU Jixin** interpreted the results and conducted the analysis. Mr. **JIANG Hao** contributed to the model construction. Dr. **ZENG Weili** and Dr. **YANG Zhao** contributed to the discussion and background of the study. All authors commented on the manuscript draft and approved the submission.

**Competing interests** The authors declare no competing interests.

(Production Editor: ZHANG Bei)

# 面向森林巡检的无人机机库选址协作部署方法

钱　龙[1]，刘继新[1,2]，江　灏[1]，曾维理[1,2]，羊　钊[1,2]

（1.南京航空航天大学民航学院，南京 211106，中国；2.空中交通管理系统全国重点实验室，南京 211106，中国）

**摘要：**针对森林巡检中复杂三维地形遮挡和大面积协同覆盖需求导致的机库部署难题，本文旨在构建一种兼顾基础设施成本与运营效率的两阶段选址协同部署框架。首先，利用数字高程模型、气象及电力数据，通过多准则决策分析方法对候选机库位置进行优化初选；随后，创新性地构建了融入地形视线阻隔、重要区域双重覆盖冗余及应急返航限制的多目标优化模型。在此基础上，引入带精英策略的非支配排序遗传算法对模型进行全局寻优。复杂森林区域的实例验证与对比结果表明，本文方法仅需11个机库即可实现92.75%的巡检覆盖率，较单目标遗传算法提升了4.36%的覆盖面积，且在40代左右即快速收敛；同时，相比传统贪婪算法成功减少了8.3%的机库建设数量。本研究证实了三维地形感知模型在复杂环境选址中的关键作用，揭示了成本预算与覆盖效率之间的边际平衡原理，为资源受限条件下的森林巡检基础设施规划提供了科学的决策依据。

**关键词：**森林巡检；无人机机库部署；多准则决策分析；地形遮挡；多目标优化

**研究亮点：**

1. 针对森林复杂环境巡检中建设成本与覆盖效率面临的权衡问题，本文提出了一种融合地理信息多准则决策与多目标精细化配置的两阶段机库协同部署范式。

2. 本文构建了一套具有三维地形感知与冗余保障的机库选址优化模型，通过数学转化突破了传统二维简化模型对山脊线“视线遮挡”的忽略，实现了对敏感目标区域的双机协同覆盖与应急安全保障。